Nuovo Cimento 56B, 47 (1968).
[8]W. Brandt and L. Eder, Phys. Rev. 142, 165 (1966).
[9]W. L. Korst and J. C. Warf, Inorg. Chem. 5, 1719 (1966).
[10]M. P. Chouinard, D. R. Gustafson, and R. C. Heckman, J. Chem. Phys. 51, 3554 (1968).
[11]T. P. Abeles, W. G. Bos, and P. J. Ouseph, J. Phys. Chem. Solids 30, 2159 (1969).
[12]D. A. L. Paul and P. C. Strangeby, in *Positron Annihilation*, edited by A. T. Stewart and L. O. Roellig (Academic, New York, 1967), pp. 417–419.
[13]C. Bussolati, S. Cova, and L. Zappa, Nuovo Cimento 50B, 256 (1967).
[14]J. E. Jackson and J. D. McGervey, J. Chem. Phys. 38, 300 (1963); J. D. McGervey, in *Positron Annihilation*, edited by A. T. Stewart and L. O. Roellig (Academic, New York, 1967), p. 144.
[15]A. Bisi, A. Fiorentini, and L. Zappa, Phys. Rev. 131, 1023 (1963).
[16]J. L. Rodda and M. G. Stewart Phys. Rev. 131, 255 (1963).
[17]C. Bussolati, A. Dapasquier, and L. Zappa, Nuovo Cimento 52B, 529 (1967).
[18]H. Kugel, E. Funk, and J. Mihelich, Phys. Letters 20, 364 (1966).
[19]W. G. Bos and H. S. Gutowsky, Inorg. Chem. 6, 552 (1967).
[20]G. G. Libowitz and J. G. Pack, J. Chem. Phys. 50, 3557 (1969).
[21]D. S. Schreiber, Phys. Rev. 137, A860 (1965).
[22]R. C. Heckman, J. Chem. Phys. 46, 2158 (1967).
[23]J. Green and J. Lee, *Positronium Chemistry* (Academic, New York, 1964), p. 39.
[24]B. Stalinski, Bull. Acad. Polon. Sci., Classe III 5, 997, (1957); 5, 1001 (1957).

PHYSICAL REVIEW B VOLUME 3, NUMBER 1 1 JANUARY 1971

Fe^{57} Nuclear Magnetic Resonance and Some Dynamical Characteristics of Domain Walls in α-Fe_2O_3 †

A. Hirai, * J. A. Eaton, ‡ and C. W. Searle
Department of Physics, University of Manitoba, Winnipeg, Manitoba, Canada
(Received 10 August 1970)

Steady-state Fe^{57} nuclear magnetic resonance (NMR) signals in α-Fe_2O_3 have been reexamined using large good-quality synthetic single crystals. It has been confirmed that strong signals originate in domain walls. The detected signal is related to the electronic loss modulated by the real part of the susceptibility of the nuclear spins, χ_n'. The total loss detected in a coil is proportional to $1+m\chi_n'$, where m is the modulation index. It is shown theoretically that for a domain wall with a wall resonance frequency $\nu_0 > \nu_N$, where ν_N is the NMR frequency, m is positive; while for a wall with $\nu_0 < \nu_N$, m is negative. This effect has been observed experimentally and correlated with domain-pattern observations, magnetization measurements, and also pulsed-NMR experimental results.

INTRODUCTION

Several years ago one of the present authors, with his co-workers, studied the characteristics of Fe^{57} nuclear magnetic resonance (NMR) signals in the weak ferromagnet α-Fe_2O_3.[1] It was concluded that the NMR signals were mainly due to nuclei within the domain walls. Their experiments, however, used polycrystalline natural samples, and detailed information on the characteristics of domain walls, for example, could not be obtained.

Another of the present authors, with his coworkers, has studied the domain structure by domain-pattern observations.[2] There now seems to be a somewhat clearer understanding of magnetic domains and domain walls in this material.

It is well known that NMR signals in ferromagnetic materials are strongly enhanced. When the enhancement of NMR signals is considered, not only the enhancement of the applied rf field, but also the back reaction of the nuclear spin system on the electronic spin system should be treated properly. Such a refined theory has been developed by Portis *et al.*[3] However, until now the validity of their results has not been carefully checked, especially in the case of domain-wall enhancement.

Therefore, it seemed worthwhile to reexamine the Fe^{57} NMR signals in α-Fe_2O_3 using good-quality synthetic single-crystal samples. The purposes of the present experiments were the following. The first experiment was to check whether or not the Fe^{57} NMR signals really come from the nuclei within the domain walls. Then, if the NMR signals do indeed come from nuclei within the domain walls, a second experiment was to test Portis's refined expression for the intensity of NMR absorption by the domain-wall enhancement mechanism. Finally, a further investigation was made to determine what particular kind of information can be obtained about domains and domain walls.

Recently several papers have appeared which treat the same subjects.[4–6] However, judging from the data on the temperature dependence of the NMR sig-

nal intensity around the Morin temperature (cf. Fig. 5), it was concluded that our crystals were better than those of the others. Indeed, as a result of this study, it has been found that the NMR signals do come from the nuclei within domain walls and that they change phase, depending on the nature of the domain walls. This experimental fact can be satisfactorily accounted for by using Portis's refined theory and making reasonable assumptions on the nature of the domain walls. Conversely, information can be obtained on the dynamical characteristics of domain walls in this material from NMR data if other supporting data are available.

EXPERIMENTAL METHODS

The single-crystal samples used in the present experiments are the same as those used in Ref. (2), where a detailed description of the crystal growth and some characteristics of the samples has been given. In the present study only pure crystals of relatively large size, about 4 g, were used. In α-Fe_2O_3, domains are very sensitive to strain-induced basal-plane anisotropy and it is not unexpected to find the domain characteristics sensitive to heat treatment. A sample (referred to as crystal A henceforth), on which we have made extensive experiments, was annealed at 1300 °C for about 48 h and then slowly cooled to room temperature (10 °C/h). For the sake of comparison, similar experiments have been performed on another sample (crystal B) which was grown in the same run as crystal A but has been subjected to no further heat treatment.

Steady-state NMR signals were taken by using a conventional frequency-modulated push-pull marginal-oscillator spectrometer. The so-called video output was plotted on an X-Y recorder by means of a boxcar integrator. Phase-sensitive detection methods, with a modulation frequency of about 14 Hz, were also used. In such experiments, to avoid any possible passage effects,[7] it is desirable to use the lowest modulation frequency and the slowest sweep possible. Though slight changes in the NMR line shape were noticed when the modulation frequency was changed, it is thought that the essential features of the present experimental results do not contain any passage effects. Thus the experimental data were analyzed by assuming that the adiabatic slow-passage condition was satisfied.

Pulsed-NMR (spin-echo) experiments were performed using a variable-frequency double-rf generator and receiver (model 6600 and plug-in model 760A) manufactured by MATEC Inc. Small external fields were applied by Helmholtz coils. In the pulsed-NMR experiments a maximum of about ± 100 Oe could be applied to the samples, while for the steady-state NMR, because of experimental inconveniences, a maximum of ± 22 Oe could be applied. All the experiments, except that of Fig. 5, were performed at room temperature. Magnetization measurements were obtained using a vibrating-sample magnetometer manufactured by Princeton Applied Research Corp.

EXPERIMENTAL RESULTS

One of the remarkable features of the present experiment was that two types of NMR signals, with opposite phases, were detected. Typical examples of the detected signals are shown in Figs. 1–4. Figures 1 and 3 are for crystal A; Figs. 2 and 4 are for crystal B. Figures 1 and 2 were obtained using direct video detection and Figs. 3 and 4 by phase-sensitive detection (which corresponds to the first derivative of the curves of Figs. 1 and 2, respectively). These data were all taken at zero external magnetic field with the rf magnetic field in the basal plane.

Figures 1 and 2 show the detected voltage at the plate of the push-pull marginal oscillator. When this signal is related to the loss in the sample coil, situated in the grid circuits, the phase should be inverted. Then, near the resonance frequency, the total loss in the sample coil is found to be proportional to $1+m\chi'_N$, where m is defined as the modulation index and χ'_N is the real part of the nuclear spin system susceptibility. From Fig. 1 it can be seen that crystal A has $m<0$ and crystal B has $m>0$. In Figs. 3 and 4 the base lines are not smooth. This is not, however, due to noise but due to the traces of wall resonances, as reported

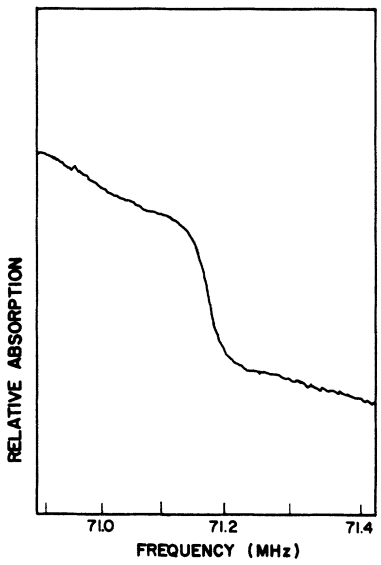

FIG. 1. Typical recorder trace of Fe^{57} NMR in α-Fe_2O_3 (crystal A) at room temperature with no applied magnetic field. Video detection was used with a boxcar integrater.

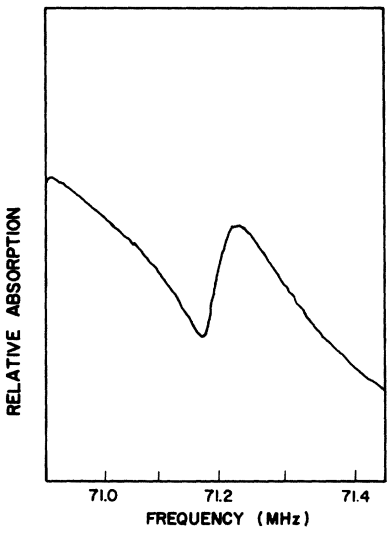

FIG. 2. Typical recorder trace of Fe^{57} NMR in α-Fe_2O_3 (crystal B). The experimental conditions are the same as in Fig. 1.

earlier by other workers.[8,9]

To test the quality of crystal A, the temperature dependence of the NMR signal intensity around the Morin temperature has been measured and the result is shown in Fig. 5. It has already been established by many workers that the NMR signal can be seen only in the temperature range where the sample exhibits weak ferromagnetism due to the Dzyaloshinski-Moriya interaction. It can be seen in Fig. 5 that the transition from the antiferromagnetic state to the weak ferromagnetic state occurs in a very narrow temperature range. This is an indication that the sample used in the present experiment is of better quality than those used by previous workers. The sign of the signal intensity corresponds to the sign of m as explained in the previous paragraph.

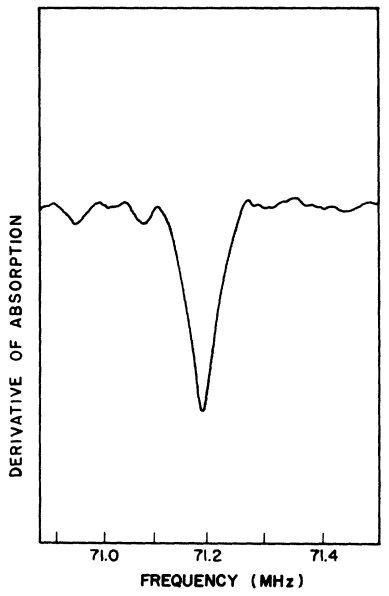

FIG. 3. Typical recorder trace of Fe^{57} NMR in α-Fe_2O_3 (crystal A) using phase-sensitive detection. The other experimental conditions are the same as in Fig. 1.

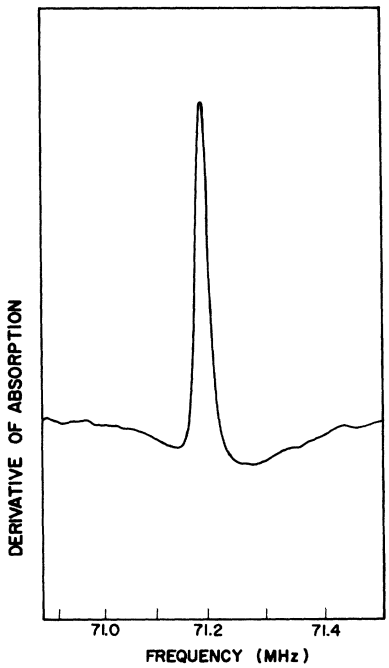

FIG. 4. Typical recorder trace of Fe^{57} NMR in α-Fe_2O_3 (crystal B) using phase-sensitive detection. The other experimental conditions are the same as in Fig. 1.

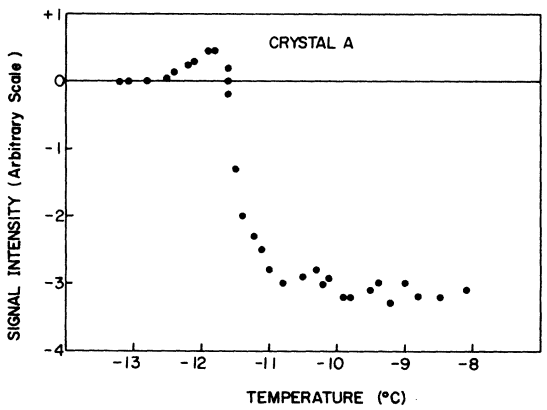

FIG. 5. Temperature dependence of the Fe^{57} NMR signal intensity around the Morin transition (crystal A).

Orientation experiments showed that only the component of the rf field in the basal plane (111) is effective in the excitation of NMR signals. No anisotropy of signal intensity within the basal plane could be found. This is undoubtedly because of the masking of the relatively weak intrinsic sixfold anisotropy within the basal plane by the anisotropy induced by random strain.

The dependences of the NMR signal intensities with respect to an externally applied magnetic field are shown in Figs. 6 and 7 for crystal A and B, respectively. These experiments were performed with the rf field H_x parallel to the external static field H_0 and both fields applied in the basal plane (111). Various other configurations are possible, but they tend to complicate the experimental situation. It should be mentioned that when H_0 is applied parallel to the c axis with H_x in the basal plane (111) the signal intensity is independent of H_0. Figures 6 and 7 show that there is a large hysteresis associated with the NMR signal intensity. It was found that the maximum field of 22 Oe provided by the Helmholtz coil was not enough to provide a symmetric hysteresis loop. This problem was eliminated by saturating the sample in either direction by superimposing ~ ± 500 Oe with a horseshoe magnet each time the Helmholtz coil provided the maximum of ± 22 Oe. This procedure provided the hysteresis curves of Figs. 6 and 7 which are almost completely symmetric. Figure 6 shows that the NMR signal changes phase (for crystal A) at H_0~ 10 Oe, where two NMR signals of opposite

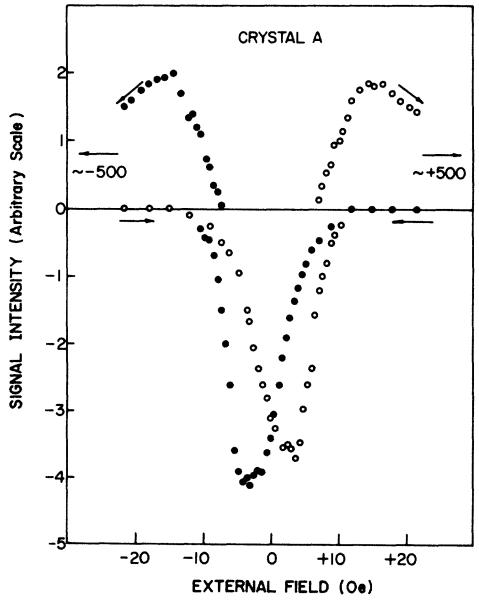

FIG. 6. Hysteresis loop of the Fe^{57} NMR signal intensity in α-Fe_2O_3 (crystal A).

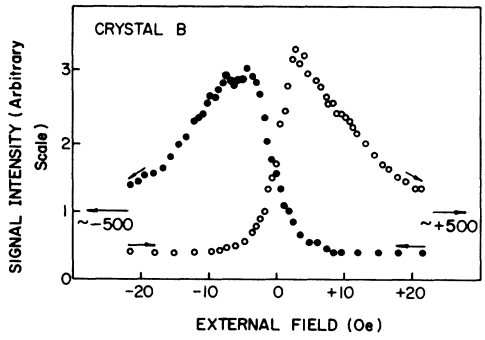

FIG. 7. Hysteresis loop of the Fe^{57} NMR signal intensity in α-Fe_2O_3 (crystal B).

phase are superposed. This superposition is more clearly demonstrated in Fig. 8. It can also be seen that the NMR signal with $m > 0$ has a narrower linewidth than the signal with $m < 0$ because the signal with $m < 0$ has already suffered from saturation broadening which will be discussed in the next section. In fact it was experimentally very difficult to obtain stable NMR signals from crystal A which was very apt to be saturated with the conventional marginal condition.

To confirm these as typical results, crystals of various kinds were trested. Almost all crystals showed NMR signals like Fig. 2 (or Fig. 4) in their untreated state. After annealing, the NMR signals changed shape to that of Fig. 1 (or Fig. 3). The NMR signal shape was returned to that of Fig. 2 (or Fig. 4) by quenching the well-annealed sample

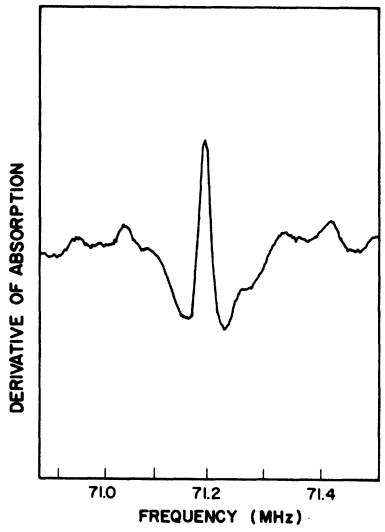

FIG. 8. An example of the recorder trace of Fe^{57} NMR in α-Fe_2O_3 showing superposition of two components with opposite phase.

from 1300 °C to room temperature. In some crystals, for example those grown near the surface in the crucible, a large component of the NMR signal with $m > 0$ could not be removed with the annealing treatment outlined above and the signal shape looked like that shown in Fig. 8.

From the hysteresis curves of Figs. 6 and 7 and the agreement between the theoretical calculations and experimental results as discussed in the next section, it is clear that the observed Fe^{57} NMR signals in α-Fe_2O_3 originate from the domain walls.

Spin-echo signals were observed from all samples but they were much weaker than what might be expected from a simple consideration of the intensity of the steady-state NMR signal. This is also a characteristic of NMR signals originating from domain walls, as shown in the next section. The hysteresis curve of the spin-echo amplitude (crystal A) as a function of H_0 is shown in Fig. 9. The relative orientation is the same as that used in the steady-state NMR. Although the pulsed-NMR apparatus was phase incoherent and could not detect the phase change of the spin-echo signal, Fig. 9 appears consistent with Fig. 6.

Use of the spin-echo method yields an enhancement factor of the applied rf field η_1. The experimental procedure was the same as that in Ref. 1, except that a single crystal with the rf field in the basal plane was used in the present experiment. The most difficult and unreliable factor of this kind of experiment is the estimation of the value of the applied rf field intensity. In the present experiment, as in the previous one, it was estimated by measuring the induced voltage in a two-turn pickup coil placed on one side of the sample coil. The spin-echo signal was maximized when the first pulse had a 1 μsec width, the second had a 2 μsec width, and the peak rf field was ~ 15 mG. This yields an enhancement factor $\eta_1 \sim 240\,000$, which is about one order of magnitude larger than the powdered case.[1]

The spin-echo decay time was about 160 μsec. Precise measurement of the spin-lattice relaxation time, which is a very complicated problem, has not been carried out at this time.

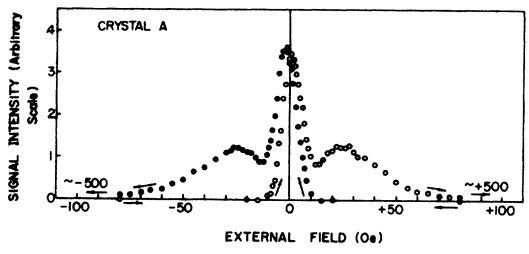

FIG. 9. Hysteresis loop of the Fe^{57} NMR spin-echo signal intensity in α-Fe_2O_3 (crystal A).

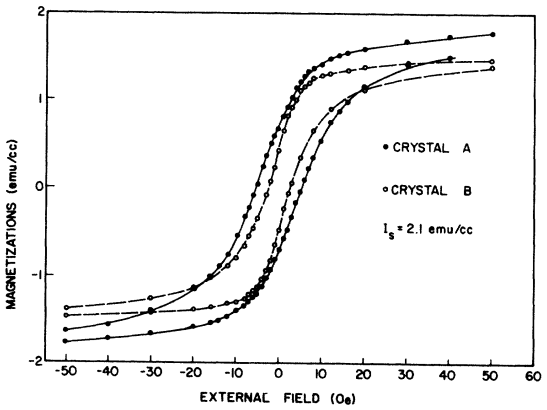

FIG. 10. The magnetic hysteresis loop in α-Fe_2O_3 (crystals A and B).

Magnetic hysteresis loops for crystal A and crystal B are shown in Fig. 10.

DISCUSSION OF EXPERIMENTAL RESULTS

In this section the two NMR signals which appear with opposite phase will be discussed in terms of Portis's refined expression for the NMR signal intensity due to domain-wall enhancement. Then values for some constants, which determine the dynamical characteristics of domain walls, will be estimated. Finally, the mutual consistency and validity of the approximations used to derive the final expressions for the NMR signal intensity will be considered.

A. Theoretical Expression for the NMR Signal Intensity by Domain-Wall Enhancement

The simplest case will be considered first. This is a two-domain particle where the domains are separated by a 180° wall, but the interaction between the electron spins and the nuclear spins will be treated properly.

Following Portis *et al.*,[3] the equation of motion for the domain wall is

$$\mu\frac{d^2z}{dt}+\beta\frac{dz}{dt}+\alpha z = 2I_S H_X - \delta U, \tag{1}$$

where z is the parameter specifying the position of the wall, μ the wall mass, β the damping constant, and α the stiffness constant. The right-hand side of Eq. (1) represents the pressure on the wall. In the first term, H_x is the external applied magnetic field and I_S the spontaneous saturation magnetization. The second term is due to the hyperfine interaction, whose energy density is given by

$$U = -(H_N/M)(\vec{\mathrm{M}}\cdot\vec{\mathrm{m}}), \tag{2}$$

where H_N is the hyperfine field, M the sublattice magnetization (in a simple ferromagnet $I_S = M$), and

m is the nuclear magnetization.

Now three special situations will be considered.

1. *Enhancement of Applied* rf *Field*

In this case we may safely neglect the pressure due to the hyperfine interaction. Then the effective rf field seen by the nucleus, H_1, is

$$H_1 \simeq H_N \frac{d\theta}{dz'} z = 2H_N I_S \frac{d\theta}{dz'} \frac{(\alpha - \mu\omega^2) - i\beta\omega}{(\alpha - \mu\omega^2)^2 + \beta^2\omega^2} H_X \,, \quad (3)$$

where θ is the angle between the electron spin within a domain wall and the spin-easy axis. For a 180° wall

$$\frac{d\theta}{dz'} \simeq \frac{1}{\delta} \sin\theta.$$

Then

$$|\eta_1| = \left|\frac{H_1}{H_X}\right| = \frac{2H_N I_S \sin\theta}{\mu\delta[(\omega_0^2 - \omega_N^2)^2 + (\beta/\mu)^2\omega_N^2]^{1/2}} \,, \quad (4)$$

where δ is the wall thickness, ω_N the NMR angular frequency, and $\omega_0 = (\alpha/\mu)^{1/2}$ the wall-resonance angular frequency.

2. *Enchancement of the Nuclear Spin-Echo Signal in a Spin-Echo Experiment*

At the moment when the spin echo appears, the oscillatory component of the semimacroscopic nuclear magnetization $m_\perp(z')$, which would be a function of z' or θ, appears perpendicular to the direction of the hyperfine field (or the direction of the electronic magnetization). This oscillatory nuclear magnetization drives the domain wall through the second term on the right-hand side of Eq. (1). This pressure is given by

$$\delta U = H_N \int_{-\infty}^{\infty} \frac{d\theta}{dz'} m_\perp(z')\, dz' \,, \quad (5)$$

and the solution of Eq. (1) is

$$z = H_N \langle m_\perp \rangle \frac{(\alpha - \mu\omega_N^2) - i\beta\omega_N}{(\alpha - \mu\omega_N^2)^2 + \beta^2\omega_N^2} \,, \quad (6)$$

where by definition

$$\langle m_\perp \rangle = \frac{1}{\delta} \int_{-\infty}^{\infty} m_\perp(z') \sin\theta\, dz'. \quad (7)$$

The oscillatory portion of the total magnetic moment per unit volume, M', can be written as

$$M' = 2I_S A z / V, \quad (8)$$

where A is the area of the wall and V the volume of the particle. The enhancement factor of the spin-echo signal is now somewhat arbitrarily defined as $\eta_2 = M'/\langle m_\perp \rangle$ which yields

$$|\eta_2| = \frac{2H_N I_S A}{V} \frac{1}{\mu[\omega_0^2 - \omega_N^2)^2 + (\beta/\mu)^2\omega_N^2]^{1/2}} \,. \quad (9)$$

It should be noted that η_2 is smaller than η_1 by the factor $A\delta/V$.

3. *Response to a Steady-State Small-Amplitude Excitation*

Following Portis *et al.* the driving pressure due to the hyperfine interaction is given by

$$\delta U = 2H_N^2(\chi_n' - i\chi_n'')z \int \left(\frac{d\theta}{dz'}\right)^2 dz' \equiv (\epsilon' - i\epsilon'')z \,, \quad (10)$$

where $\chi_n = \chi_n' - i\chi_n''$ is the rf susceptibillity of the nuclear spins. Then the solution of Eq. (1) is

$$z = \frac{2I_S H_X}{(\alpha - \epsilon' - \omega^2\mu) + i(\omega\beta + \epsilon'')} \,. \quad (11)$$

The energy dissipation can be written as

$$P = \tfrac{1}{2}\,\mathrm{Re}(2i\omega z I_S H_X)$$

$$= 2\omega_N I_S^2 H_X^2 \frac{(\omega\beta + \epsilon'')}{\mu^2(\omega_0^2 - \omega_N^2 - \epsilon'/\mu)^2 + (\omega\beta + \epsilon'')^2} \,. \quad (12)$$

If the following conditions are satisfied,

$$1 \gg \frac{2}{|\omega_0^2 - \omega_N^2|} \frac{\epsilon'}{\mu} > \frac{\epsilon''}{\omega\beta} \,, \quad (13)$$

then Eq. (12) can be simplified to

$$P \simeq P_0[1 + m\chi_n'] \quad (14)$$

with

$$P_0 = 2\omega_N^2 I_S^2 H_X^2 \frac{\beta}{\mu^2} \frac{1}{(\omega_0^2 - \omega_N^2)^2} \,, \quad (14')$$

$$m = \frac{1}{\omega_0^2 - \omega_N^2} \frac{1}{\mu} 2H_N^2 \int \left(\frac{d\theta}{dz'}\right)^2 dz' \,. \quad (14'')$$

These equations clearly show that the NMR has a dispersionlike character and that its modulation index m may change its sign depending on whether ω_0 is larger or smaller than ω_N.

B. Comparison with Experimental Results

The theoretical results obtained above will now be compared with the experimental data. P, the power absorption in the resonance coil due to the experimental sample, was calculated above. The experimentally measured quantity, however, is the change of the plate current of the push-pull marginal oscillator. The detected signal is assumed to be proportional to the power absorption (the operation of the marginal oscillator is very complicated as far as this statement is concerned and the statement is therefore only roughly correct). In addition, the theoretical calculations assumed one 180° domain wall in a ferromagnetic particle, while the experimental samples were large α-Fe_2O_3 single crystals which are weak (canted) ferromagnets. However, domain-pattern observations indicate that most of the domain walls in α-Fe_2O_3 are 180° walls[2]; and further if it is assumed that the

canting angle does not change in the domain wall, the theoretical calculations can be applied to the present situation.

Comparing Figs. 6 and 7 with Eq. (14) it is apparent that the domain walls can be classified into two types according to the sign of m. One type, called a movable wall, is predominant in well annealed samples around zero external field. This type of domain probably forms in order to reduce the magnetostatic energy and should exist even in perfect crystals. It has a small stiffness constant, α, and a correspondingly small resonance frequency

$$\nu_0 (\nu_0 < \nu_N = 71.2 \text{ MHz}).$$

This wall is swept out easily by a small external magnetic field of the order of 10 Oe (a precise value of this critical field could be obtained by treating the demagnetization factor carefully in both the experiment and calculation; however, the demagnetization field for these irregular-shaped crystals should be on the order of $\frac{4}{3}\pi I_S = 8.8$ Oe which is in agreement with the 10-Oe field needed to remove this type of domain). The second type of wall is one that is trapped by some kind of imperfection in the crystal. This type is rather difficult to sweep out with an external static field as can be seen in Fig. 9 where at least 100 Oe was needed to sweep out this wall. This wall stiffness constant is so large that $\nu_0 > \nu_N$.

Some of the constants which characterize domain-wall motion will be considered somewhat quantitatively to see if this interpretation of the experimental results seems reasonable. The following experimental constants,

$$\delta = 4\text{–}10\ \mu \simeq 7\times10^{-4} \text{ cm},$$

$$l = 50\text{–}150\ \mu \simeq 1\times10^{-2} \text{ cm},$$

are taken from the data of Eaton and Morrish.[2] From the magnetization data (cf. Fig. 10) the initial susceptibility $\chi_0 \simeq 0.1$ emu/cm^3 Oe and the saturation magnetization $I_S = 2.1$ emu/cm^3 are obtained. Then using the standard formula[10]

$$\mu = 1/8\pi\gamma_0^2\delta = 1.9\times10^{-13} \text{ g/cm}^2,$$

$$\alpha = 4I_S^2/\chi_0 l = 1.8\times10^4 \text{ g/cm}^2 \text{ sec}^2.$$

it is found that

$$\nu_0 = \frac{\omega_0}{2\pi} = \frac{1}{2\pi}(\alpha/\mu)^{1/2} = 49.0 \text{ MHz}. \quad (15)$$

This calculated value of ν_0 is indeed smaller than $\nu_N = 71.2$ MHz as expected for the movable walls. Domain structures, with typically the same dimensions as the easily removable domain structures, have been observed which show a greater resistance to applied magnetic fields and some are still present in fields exceeding 100 Oe. The behavior of these walls also appears to have some connection with internal strain and therefore these walls appear to be responsible for the positive-phase NMR signals. The initial susceptibility associated with the trapped walls is taken from Fig. 10 for $H \sim 50$ Oe which results in

$$\chi_0 \simeq 0.2\times10^{-2} \text{ emu/cm}^3 \text{ Oe}.$$

This value is still more than two orders of magnitude larger than the background antiferromagnetic susceptibility and should be a reasonable estimation. All other constants are assumed to be the same as those of the movable walls. Then for the trapped walls

$$\alpha = \frac{4I_S^2}{\chi_0 l} = 90\times10^4 \text{ g/cm}^2\text{sec}^2$$

and

$$\nu_0 = \omega_0/2\pi = \tfrac{1}{2}(\alpha/\mu)^{1/2} = 346 \text{ MHz}.$$

This calculated value of ν_0 is indeed greater than $\nu_N = 71.2$ MHz as expected for this type of wall.

β is now estimated from the ferromagnetic resonance linewidth ΔH. The smallest value reported to date is $\Delta H \sim 50$ Oe at the microwave frequency of 24 GHz.[11] Using the standard relation $\beta = 2\Delta H I_s/\delta(\gamma_0 H_{res})$

$$\beta = 2.0\times10^{-6} \text{ g/cm}^2\text{sec}.$$

A combination of these values and Eq. (4) yields $|\eta_1| \sim 1.6\times10^5$, which agrees with the experimental value of 240 000.

In deriving Eq. (14), we have assumed [cf. inequality (13)] that the NMR line is inhomogeneously broadened and that the effective (enhanced) rf field is sufficiently strong so that the imaginary part of the nuclear susceptibility (χ_n'') is already well saturated, while the real part, χ_N', still survives. This is the saturation characteristic of inhomogeneously broadened lines.[12] This assumption will now be checked. The total inhomogeneously broadened NMR linewidth $\Delta\nu_0$, from Figs. 3 and 4, is of the order of 70 kHz. The homogeneous linewidth $\Delta\nu$ is very difficult to estimate. However, if we naively assume that it is given from the spin-echo decay time by the relation $\Delta\nu = 1/2\pi T_2$, then the homogeneous linewidth is of the order of 1 KHz for $T_2 = 160$ μsec. $\Delta\nu_0$ is then about two orders of magnitude larger than $\Delta\nu$. These two values of $\Delta\nu_0$ and $\Delta\nu$ should be compared with the effective rf field (expressed in units of frequency) $(\gamma_N/2\pi)\eta_1 H_x$. The value of H_x for the marginal oscillator is of the order of several mOe. Then $(\gamma_N/2\pi)\eta_1 H_x$ is of the order of 100 kHz for $H_x = 3$ mOe, which is very much larger than $\Delta\nu$ and even larger than $\Delta\nu_0$. This shows that for the movable wall the inhomogeneously broadened NMR line has already begun to saturate. On the other hand, for a trapped wall, the enhancement factor could reasonably be one order of mag-

nitude smaller than that for the movable wall, which might imply that the NMR signals due to this type of wall are not saturated yet. This may be the reason why the signal in Fig. 4 is narrower than that of Fig. 3 and explains the line shape of Fig. 8. Finally, with the numerical values listed above it is easy to check that the inequalities of relation (13) are valid for this material.

From Fig. 5 it is apparent that the portion of the sample with the least strain goes through the Morin transition at $-11.5\,^{\circ}C$ and that portions which contain more strain have a lower transition temperature.

In summary, Fe^{57} NMR signals originate from nuclei within domain walls. Walls in α-Fe_2O_3 can be classified into two groups. One is an intrinsic movable wall, while the other wall is trapped by imperfections. Various dynamical quantities have been estimated for these walls and have been shown to be consistent with all the available data.

ACKNOWLEDGMENTS

We wish to acknowledge the helpful comments of Professor A. H. Morrish and the hospitality that the Department of Physics at the University of Manitoba extended to one of us (A. H.).

---

†Research for this paper supported by the National Research Council of Canada, Grant No. A2883.

*On leave from Kyoto University, Kyoto, Japan.

‡Present address: Department of Physics, Trent University, Peterborough, Ontario, Canada.

[1]M. Matsuura, H. Yasuoka, A. Hirai, and T. Hashi, J. Phys. Soc. Japan 17, 1147 (1962).

[2]J. A. Eaton, A. H. Morrish, and C. W. Searle, Phys. Letters 26A, 520 (1968); J. A. Eaton and A. H. Morrish, J. Appl. Phys. 40, 3180 (1969).

[3]A. C. Gossard, A. M. Portis, M. Rubinstein, and R. H. Lindquist, Phys. Rev. 138A, 1415 (1965).

[4]D. H. Anderson, Phys. Rev. 151, 247 (1966).

[5]B. Sedlack, Czech. J. Phys. 18B, 1374 (1968).

[6]A. V. Zalasskii, I. S. Zheludev, and R. A. Voskanyan, Zh. Eksperim. i Teor. Fiz. Pis'ma V Redaktsiyu 9, 242 (1969) [Soviet Phys. JETP Letters 4, 242 (1969)].

[7]See, e.g., D. L. Cowan and L. W. Anderson, Phys. Rev. 135, A1046 (1964).

[8]E. L. Boyd, J. I. Budnick, L. J. Bruner, and R. J. Blume, J. Appl. Phys. 33, 2484 (1962).

[9]B. Sedlack and H. Szydlowski, Czech. J. Phys. 17B, 889 (1967).

[10]See, e.g., S. Chikazumi and S. H. Charap, *Physics of Magnetism* (Wiley, New York, 1964); C. Kittel and J. K. Galt, in *Solid State Physics*, edited by F. Seitz and C. Turnbull (Academic, New York, 1956), Vol. 3.

[11]A. H. Morrish and C. W. Searle, in *Proceedings of the International Conference on Magnetism, Nottingham*, 1964 (The Institute of Physics and The Physical Society, London, 1964), p. 574.

[12]A. M. Portis, Phys. Rev. 100, 1219 (1955); see also A. Abragam, *The Principles of Nuclear Magnetism* (Clarendon, London, 1961).